

## **THEORY OF EMANATION THERMAL ANALYSIS VII: THERMOSTIMULATED INERT GAS RELEASE AS INFLUENCED BY THE ENERGY SPECTRUM OF THE DEFECT SITES IN SOLIDS**

A.V. SHELEZNOV and I.N. BECKMAN

*Department of Radiochemistry and Chemical Technology, Moscow State University,  
199 234 Moscow (U.S.S.R.)*

V. BALEK

*Nuclear Research Institute, 256 68 Řež (Czechoslovakia)*

(Received 2 June 1988)

### **ABSTRACT**

The results are given of the investigation into the influence of the energy spectrum of defect sites in solids occupied by inert gas atoms (used as the label of solid samples) on the thermostimulated gas release rate curves. The model curves of the temperature dependences of the inert gas release were investigated using several methods, such as the method of functional scales, the analysis of the temperature dependences of the inert gas release effective activation energy  $E_{ef}(T)$  and the analysis of the dependences of the pre-exponential factor  $\ln k_0$  on the energy  $E_{ef}$ .

### **INTRODUCTION**

In previous papers [1,2], we have analysed the influence of the inertia and other characteristics of the ETA apparatus on the curves of the inert gas release from solid samples. The aim of this paper is to investigate the influence of the bond between the inert gas atoms and the defect sites on the temperature dependence of the thermostimulated inert gas release (TGR curves).

Several methods can be used for the analysis of the model TGR curves; the method of linearization by means of functional scales; the analysis of the temperature dependences of the effective activation energy  $E_{ef}$  of the gas release; and the analysis of the dependence between the pre-exponential factor  $\ln k_0$  and  $E_{ef}$  in the fundamental equation for the thermostimulated release rate of the gas from solids.

*Phenomenological description of the thermostimulated inert gas release assuming a spectrum of bond energies between the inert gas and the defect sites in the solid*

Let us suppose a solid sample labelled by an inert gas, such as radon or krypton, which is trapped in various defect sites, where  $N_i$  is the number of sites of the  $i$ th type,  $E_i$  is the energy of the bond between the inert gas label and the defect sites of the  $i$ th type and  $n_i$  is the number of inert gas atoms located on the defect sites of the  $i$ th type. The sample contains  $m$  types of defects.

For characterization of the solids labelled by inert gas before the sample heating, we use the energy spectrum  $N(E)$  of the defect sites, and the energy spectrum  $n(E)$  of the inert gas in the solid. In the case of total occupation of the defect sites by the inert gas, the spectra  $N(E)$  and  $n(E)$  are identical. This case is analysed in the present paper.

Let us suppose that the inert gas release can be described by a first-order reaction mechanism, determined by the activation energy,  $E_i$ , then the time dependence of the inert gas flow  $J(t)$  from the sample heated at constant heating rate can be expressed

$$J = \frac{d\theta_i^*}{dt} = k_{0,i} \exp\left(-\frac{E_i}{RT}\right) \theta_i^* \quad (1)$$

where  $\theta_i^*$  is the dimensionless expression for the number of inert gas atoms located on the  $i$ th type sites, normalized to the total number of the defects  $N$  where  $N = \sum_{i=1}^m N_i$ . The total inert gas flow  $J$  from the sample is

$$J = \frac{d\theta}{dt} = \sum_{i=1}^m k_{0,i} \exp\left(-\frac{E_i}{RT}\right) \theta_i^* \quad (2)$$

where  $\theta = \sum_{i=1}^m \theta_i^* = 1/N \sum_{i=1}^m N_i$  is the complete occupation of the sites by the inert gas.

Let  $\phi_i = N_i/N$  be the proportion of the potential sites of the  $i$ th type normalized to the total number of defects of the  $i$ th type. Then we can write eqn. (2) using the parameter  $\phi_i$  as follows

$$\frac{d\theta}{dt} = \sum_{i=1}^m k_{0,i} \exp\left(-\frac{E_i}{RT}\right) \phi_i \theta_i \quad (3)$$

In the case of the continuous spectrum of the activation energies of inert gas release, for the inert gas flow  $J$

$$J = \frac{d\theta}{dt} = -k_{ef} \theta = \int_0^\theta k_0(\theta^*) \exp\left(-\frac{E(\theta^*)}{RT}\right) d\theta^* \quad (4)$$

and after substituting  $d\theta^* = \theta d\phi$  we obtain

$$J = \frac{d\theta}{dt} = - \int_0^1 k_0(\phi) \exp\left(-\frac{E(\phi)}{RT}\right) \theta(\phi) d\phi \quad (5)$$

The experimental conditions of the constant heating rate are taken into account by including  $T = T_0 + \beta t$ , where  $T_0$  is the onset temperature and  $\beta$  is the heating rate ( $\text{K s}^{-1}$ ).

The solution of eqn. (3) can be written in the form

$$J(t) = \sum_{i=1}^m \theta_{i,0} k_{0,i} \exp\left(-\frac{E_i}{RT}\right) \exp(\tau_i) \quad (6)$$

where the integral time  $\tau_i = (k_{0,i} E_i / \beta R) \{ -(\exp(\xi)/\xi) + \mathbf{Ei}(\xi) \}$ , the integral exponential function  $\mathbf{Ei}(\xi) = \int_{-\infty}^{\xi} (\exp(t)/t) dt$  and  $\xi$  changes from  $E/R(T_0 + \beta t)$  to  $E/RT_0$ .

#### ANALYSIS OF THE MODEL DEPENDENCES OF INERT GAS RELEASE RATE

##### *The method of functional scales [2]*

The thermostimulated gas release (TGR) curves can be linearized by means of the functional scales calculated for various mechanisms of inert gas release and for various inert gas concentration profiles in the samples. In this paper, a first-order reaction mechanism is assumed for the TGR. When the energy spectrum  $n(E)$  is characterized by a single value of the activation energy, a simple straight line results from the plot of the functional scale  $U$  against  $1/T$ . The value of the activation energy can be determined from the slope of this line, and the frequency factor  $k_0$  can be determined from the intersection of the line with the  $y$ -axis. When the  $J(t)$  curve does not correspond to the first-order reaction mechanism determined by a single value of the activation energy, a non-linear curve results in the functional scale. The deviation of the curve from a straight line can be used to estimate the inert gas release mechanism. The functional scales corresponding to other mechanisms of gas release are subsequently used, and parameters of the initial energy spectrum are determined from the slopes of the respective curves.

##### *The analysis of the temperature dependence of the effective activation energy $E_{\text{ef}}$ of the inert gas release*

In order to analyse the temperature dependences of  $E_{\text{ef}}$ , the values of the effective diffusion constant were first determined at every point on the experimental curve  $J(t)$ . The effective diffusion constant  $k_{\text{ef}}$  can be expressed

$$k_{\text{ef}} = \frac{J(T)}{\theta T} = \frac{J(T)/F}{1 - 1/F \int_{T_0}^{T_r} J(T)} \quad (7)$$

where  $F = \int_{T_0}^{T_F} J(T) dT$  is the area of the peak on the TGR curve and  $T_0$  and  $T_F$  are the onset and final temperature of the heating respectively. The calculated  $\ln k_{ef}$  values were plotted against  $1/T$  at every point on this curve; and the activation energy  $E_{ef}$  and  $k_{0,ef}$  were evaluated. Subsequently, the temperature dependences of the plots  $E_{ef}$  against  $T$  and  $k_{0,ef}$  against  $T$  were constructed. On the basis of these plots, the spectrum of the activation energy of the inert gas release was investigated. The principles are pointed out below:

- (a) when the spectrum consists of a single activation energy, the plot of  $E_{ef}$  against  $T$  is linear and parallel to the x-axis; and
- (b) when the spectrum consists of several values of activation energy, the plot of  $E_{ef}$  against  $T$  is a non-linear decreasing function, which is just decreasing when the energy values are difficult to distinguish, and has a minimum when the energy values are clearly distinguished.

We shall demonstrate the application of this method in the analysis of the model TGR curves, assuming that the energy spectrum consists of two discrete lines  $E_1$  and  $E_2$ , where  $E_1 < E_2$ .

Taking into account the fact that the total flow  $J = J_1 + J_2$  and  $\theta = \theta_1^* + \theta_2^*$ , we obtain, by logarithmization,

$$\ln k_{ef} = \ln(k_1\theta_1^* + k_2\theta_2^*) - \ln(\theta_1^* + \theta_2^*) \quad (8)$$

After deriving eqn. (8), we obtain the expression for the slope of the plot in the coordinates  $\ln k_{ef}$  versus  $1/T$

$$\frac{\partial \ln k_{ef}}{\partial(1/T)} = \left[ \frac{-\frac{E_1}{R}J_1 - \frac{E_2}{R}J_2 + \frac{T^2}{\beta}(k_1J_1 + k_2J_2)}{(J_1 + J_2)} \right] - T^2 \frac{k_{ef}}{\beta} \quad (9)$$

at the onset of the heating run where  $J_2 \rightarrow 0$ , we can write

$$\frac{\partial \ln k_{ef}}{\partial(1/T)} = -\frac{E_1}{R} + \frac{T^2}{\beta}(k_1 - k_{ef}) \quad (10)$$

As  $(k_1 - k_{ef}) \geq 0$ , we can use eqn. (10) for estimating the value of  $E_1$ . It can be seen from eqn. (9), that several energy lines which may be superimposed in the case of a multiple energy spectrum, cause an increase in the value of  $E_{ef}$  at the onset of heating.

After heating to higher temperatures, when  $J_1 \rightarrow 0$ , i.e. when the inert gas located at sites of energy  $E_1$  has been released, we can write

$$\partial \ln k_{ef} / \partial(1/T) = -E_2/R \quad (11)$$

which means that at higher temperatures, the  $E_{ef}$  value increases and tends to  $E_{ef} = E_2 \geq E_1$ .

Consequently, the  $E_{ef}$  values obtained at low temperatures, i.e. at the beginning of the heating run, can be considered as  $E_{ef} \approx E_1$ , whereas the

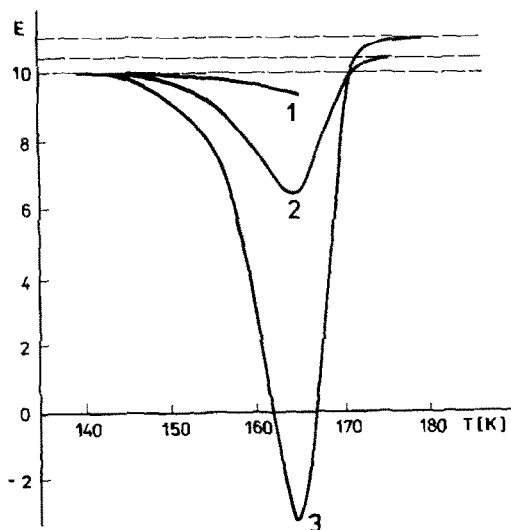


Fig. 1. Temperature dependences of the effective activation energy  $E_{ef}$  of the inert gas diffusion calculated at every point of the model TGR curves corresponding to the discrete energetic spectrum characterized by Fig. 3. (Curves 1–3 correspond to the schemes 1(a)–(c), respectively.)

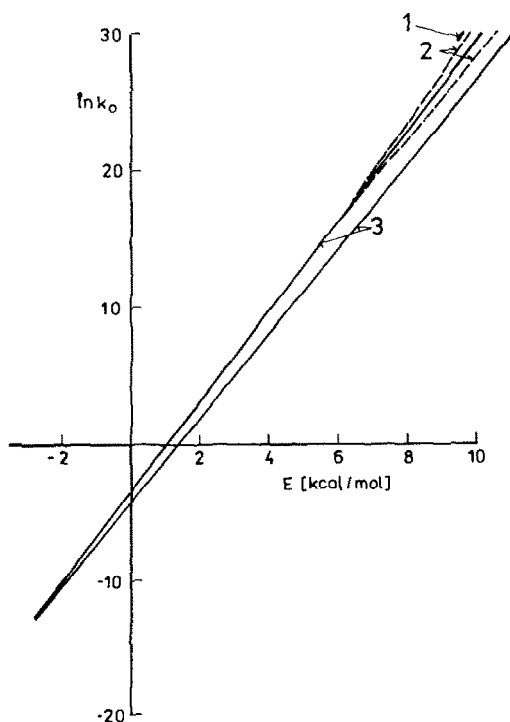


Fig. 2. The dependence of  $\ln k_0$  on the effective activation energy of the inert gas diffusion  $E_{ef}$  calculated for the solid sample characterized by the discrete energy spectra demonstrated in Fig. 3.

values  $E_{ef}$  at the end of the heating run are  $E_{ef} = E_2$ , assuming that at higher temperatures the inert gas release is determined only by the activation energy  $E_2$ . (Examples of the dependences between  $E_{ef}$  and temperature for two discrete energy spectra are given in Fig. 1).

*The analysis of the dependences of  $\ln k_0$  on  $E_{ef}$  (the compensation effect)*

In the analysis of the temperature dependences of  $\ln k_{ef}$  demonstrated in the previous section, it is usually supposed that the parameters  $\ln k_0$  and  $E$  are mutually independent. However, in several cases a dependence does exist, for example when the experimental inert gas release curves  $J(t)$  have a complex shape, and in the case of the application of different inert gases for labelling solids, etc.

In the simple case of the  $J(t)$  peak, the dependence of  $\ln k_0$  on  $E_{ef}$  is represented in Fig. 2 by a point. In the case of a complex peaked curve, it is a smoothly rising curve tending to a value of  $E$  corresponding to the onset of the energy spectrum. As is obvious from Fig. 2, in the case of the  $J(t)$  curve where two peaks are well separated, the dependence of  $\ln k_0$  on  $E_{ef}$  consists of two parts starting at one point and tending to the respective limit values of the energy spectrum (see Fig. 2). Briefly, we can state that this method makes it possible to reveal the fine structure of the spectrum  $n(E)$ .

## MATHEMATICAL MODELLING OF THE THERMOSTIMULATED GAS RELEASE CURVES

*Description of the computer program*

The program TGR (thermostimulated gas release) was written in FORTRAN and a personal computer was used for the computation of the model curves. This program is suitable for evaluating curves resulting from various methods of thermal analysis based on the measurement of the gas release, e.g. evolved gas analysis (EGA), emanation thermal analysis (ETA), etc.

The program enabled us to obtain the curves of the thermostimulated inert gas release (TGR curves) from solid samples of various shape, taking into account several distribution profiles of the gas in the sample, various heating regimes (linear, parabolic, etc.) and various mechanisms of the gas release (e.g. first- and second-order reactions, reversible or irreversible reactions). The methods mentioned above were used for the model TGR curves.

*Computing the model TGR curves and their analysis*

The model TGR curves were computed and subsequently analysed in several steps as follows.

1. In the first step, the data determining the measured system are stored in the computer memory (the shape and size of the sample, the potential energy spectrum of the defect sites  $N(E)$ , the distribution of the defect sites in the sample, etc.) The trapping of the inert gas atoms by the solid, i.e. the influence of the labelling, was subsequently analysed, assuming various types of defect sites of both limited and unlimited capacity. (The labelling process of solids consisted of inert gas diffusion at various temperatures and pressures).

2. In the second step, the model TGR curves were computed. Various initial temperatures, heating regimes and mechanisms of inert gas release from the solids were assumed during computation. In the case of a constant heating rate, the analytical dependences were used, whereas for non-linear regimes, numerical algorithms were used for solution of the differential equation. In this way, the time and temperature dependences of the amount of gas released from the sample and the inert gas release curves (TGR curves) were computed.

3. In the third step, the model curves obtained were analysed using the methods described above. The computed model curves were re-plotted in the functional scales, the parameters of the thermostimulated inert gas diffusion and the temperature dependences of these parameters were determined. The most appropriate methods for the analysis of the model TGR curves were used, enabling us to determine the energy stages and the topology of the inert gas label in the solid.

## RESULTS OF THE MATHEMATICAL MODELLING AND ANALYSIS OF THE TGR CURVES

Schemes of the energy spectra  $n(E)$  of the defect sites in the solids considered during the mathematical modelling are demonstrated in Fig. 3. In Fig. 3–6, the spectrum characterized by two activation energy values  $E_1$  and  $E_2$  is shown, assuming the same occupation of the respective defect sites by the inert gas ( $\theta_1 = \theta_2$ ). In Figs. 4–6, the spectra shown are assumed to have the same  $E_1$  but different values of  $E_2$ . Typical curves of the temperature dependences of the inert gas release from solids are demonstrated in Fig. 7. It is obvious from Fig. 7 that the dependences are single peaked curves, irrespective of whether one or two activation energy values are considered in the discrete spectrum. A higher symmetry was observed in the case where the energy spectrum has two lines. However, when the method of the analysis of temperature dependences,  $\ln k_0$  versus  $T$  and  $E_{ef}$  versus  $T$ , was used, we found the influence of both values of activation energy in the spectrum (see Fig. 1). In Fig. 1, the influence of energy lines in the spectrum differing by only 1% can be seen. A difference in the energy lines of 4% is more obvious (see Fig. 8). The values of  $E_1$  and  $E_2$  can be

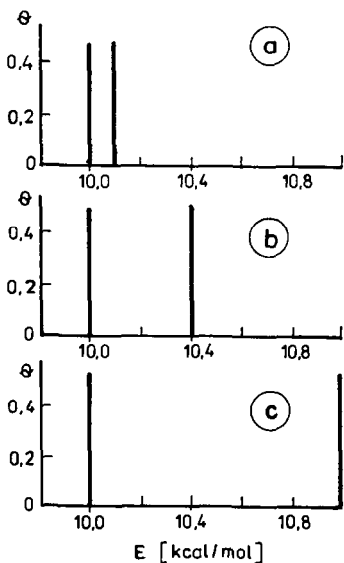


Fig. 3. Schematic diagrams of the discrete energy spectra  $n(E)$  of the solid state defect sites taking part in the inert gas diffusion. Two different energy values  $E_1$  and  $E_2$  of the effective activation energy of inert gas diffusion and the equal occupation of the defect sites by the inert gas  $\theta_1 = \theta_2 = 0.5$  are supposed:

- (a)  $E_1 = 10.0 \text{ kcal mol}^{-1}$ ,  $E_2 = 10.1 \text{ kcal mol}^{-1}$ ;  
 (b)  $E_1 = 10.0 \text{ kcal mol}^{-1}$ ,  $E_2 = 10.4 \text{ kcal mol}^{-1}$ ; and  
 (c)  $E_1 = 10.0 \text{ kcal mol}^{-1}$ ,  $E_2 = 11.0 \text{ kcal mol}^{-1}$ .

determined from the dependences in Fig. 8 using the method of the analysis of the dependences of  $E_{ef}$  on temperature, which readily enabled us to determine  $E$  values differing by 10%. Figure 2 demonstrates the dependences of  $\ln k_0$  on  $E_{ef}$  in the cases considered in the scheme in Fig. 5 (a continuous exponential-like spectrum). It can be concluded that the experimental curves fitted on the basis of the monoenergetic approximation may lead to errors. In Figs. 9A–D, the results of the method of functional scales used for the linearization of the model TGR curves are shown. Various energies in the spectra were considered, shown schematically in Figs. 3–6. A first-order reaction was assumed in the construction of the plots shown in Figs. 9A–D. It is obvious from Fig. 9A that, in the low temperature range, linear dependences were obtained and the values of  $E_{ef}$  were determined from the slopes. The break in the plot in the high temperature region indicates the existence of more than one energy value in the discrete spectrum  $n(E)$ . If the difference in the  $E$  values is high enough, the  $E_2$  value can be determined from the high temperature part of the slope.

Another problem analysed in this paper is that of the differences in the TGR curves caused by the fact that inert gas atoms are trapped at the defect sites of two lines of the energy spectrum having different intensities. During



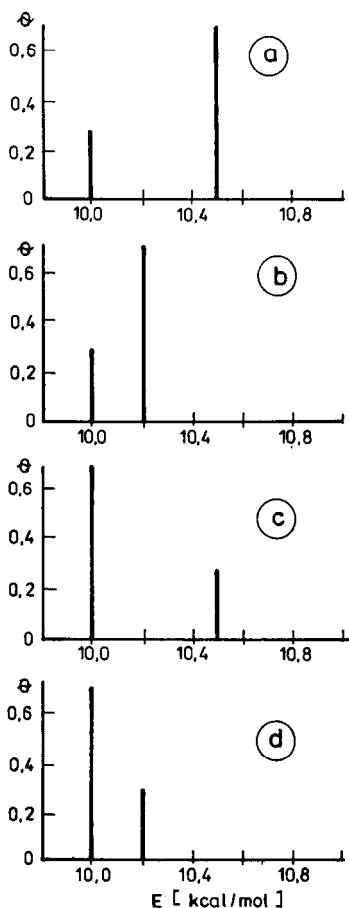


Fig. 4. Schematic diagrams of the discrete energy spectra  $n(E)$  of the solid state defect sites taking part in the inert gas diffusion. Two different energy values  $E_1$  and  $E_2$  of the effective activation energy and different occupation  $\theta_1$  and  $\theta_2$  of the defect sites by the inert gas are supposed:

- (a)  $E_1 = 10.0 \text{ kcal mol}^{-1}$ ,  $\theta_1 = 0.3$ ;  $E_2 = 10.5 \text{ kcal mol}^{-1}$ ,  $\theta_2 = 0.7$ ;  
 (b)  $E_1 = 10.0 \text{ kcal mol}^{-1}$ ,  $\theta_1 = 0.3$ ;  $E_2 = 10.2 \text{ kcal mol}^{-1}$ ,  $\theta_2 = 0.7$ ;  
 (c)  $E_1 = 10.0 \text{ kcal mol}^{-1}$ ,  $\theta_1 = 0.7$ ;  $E_2 = 10.5 \text{ kcal mol}^{-1}$ ,  $\theta_2 = 0.3$ ; and  
 (d)  $E_1 = 10.0 \text{ kcal mol}^{-1}$ ,  $\theta_1 = 0.7$ ;  $E_2 = 10.2 \text{ kcal mol}^{-1}$ ,  $\theta_2 = 0.3$ .

the modelling, the results of which are shown in Fig. 9B, the differences between the energy lines varied, as did the contributions of the individual energies in the spectrum.

As in the previous example reported in this paper, the equal values of  $E_1$  were determined from the low temperature part of the straight line. From Fig. 9B it can be seen that the slopes of the dependences do not essentially differ, whereas the intercepts of the curve on the  $y$ -axis indicate that the values of  $k_0$  do differ.

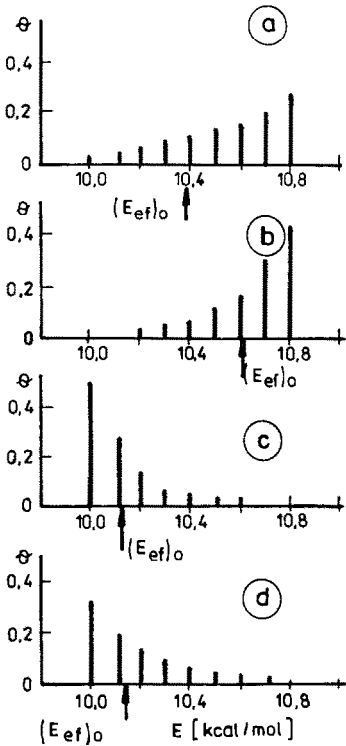


Fig. 5. Schematic diagrams of the continuous energy spectra  $n(E)$  of the solid state defects taking part in the inert gas diffusion. The spectra are approximated by exponential curves of various curvature  $a$ , as follows: (a)  $a = 0.3$ ; (b)  $a = 0.6921$ ; (c)  $a = -0.6921$ ; and (d)  $a = -0.3$ .

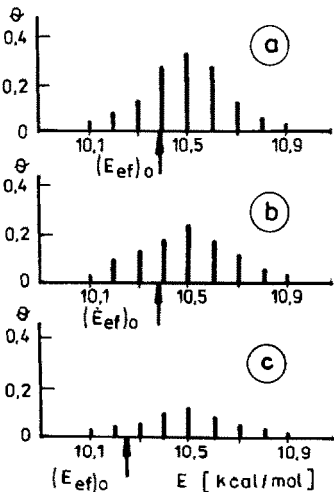


Fig. 6. Schematic diagrams of the continuous energy spectra  $n(E)$  of the solid state defects taking part in the inert gas diffusion. The spectra are approximated by the normal distribution curve and by the equal energy values  $E = 10.5 \text{ kcal mol}^{-1}$ . The dispersity  $\sigma$  of the normal distribution curve is as follows: (a)  $\sigma = 1.2$ ; (b)  $\sigma = 1.8$ ; and (c)  $\sigma = 4$ .

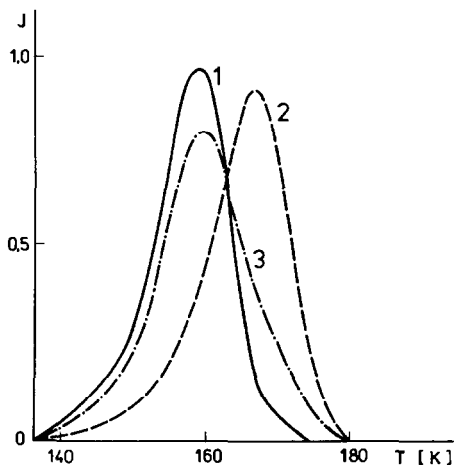


Fig. 7. Model curves of the temperature dependences of the thermostimulated inert gas release (TGR curves) for the selected cases of the discrete energy spectra: curves 1 and 2 correspond to the discrete energy spectra of the single energy value  $E_1 = 10.0$  and  $10.5$  kcal mol $^{-1}$ , respectively; curve 3 corresponds to the spectrum characterized by two discrete energy values  $E_1 = 10.0$  kcal mol $^{-1}$  and  $E_2 = 10.5$  kcal mol $^{-1}$ . In the modelling, the heating rate  $2.0$  K s $^{-1}$  and the pre-exponential factor  $10^{13}$  s $^{-1}$  were considered.

It can be stated that the  $E_{ef}$  values in the low temperature range are close to the minimum value  $E_1$  and depend very little on the concentration of the inert gas in the respective defect sites.

The influence of the continuous energy spectrum on the TGR curves was also analysed in this paper. Figure 5 shows the continuous energy spectrum

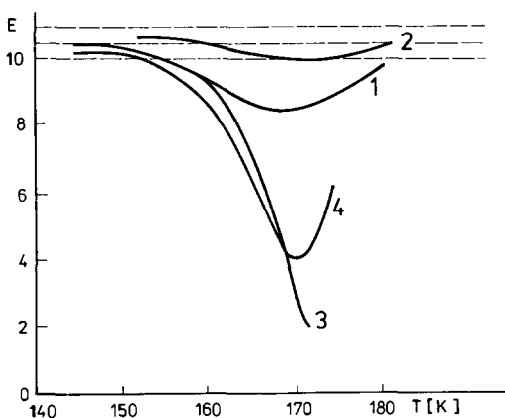


Fig. 8. Temperature dependences of the effective activation energy  $E_{ef}$  of the inert gas diffusion calculated at every point of the model TGR curves corresponding to the continuous energy spectrum approximated by the exponential curves in Fig. 5. (Curves 1–4 correspond to the schemes 5(a)–(d), respectively).

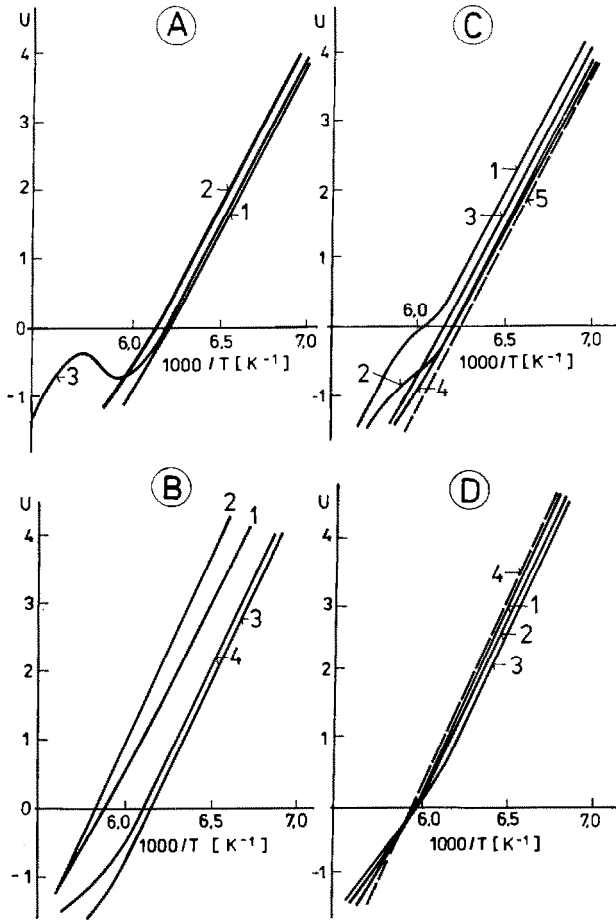


Fig. 9A-D. The functional plots of  $U$  against reciprocal value of temperature ( $1/T$ ), computed for the model curves of thermostimulated inert gas release from solid samples characterized by different energy spectra as shown in Figs. 3-6, respectively. The dotted lines in Figs. 9C and 9D correspond to the curves representing the spectrum approximated by the single energy value  $E_{cf} = 10.5 \text{ kcal mol}^{-1}$ .

which can be described by the exponential equation

$$\theta_i(E) = \exp\left(a \frac{E - E_o}{\Delta E}\right) \quad (12)$$

where  $E_o$  is the energy of the spectrum onset and  $\Delta E$  is the discretization interval. The amounts of gas trapped in the individual sites can be expressed in the normalized form  $\sum_i \theta_i(E) = 1$ . The parameter  $a$  characterizes the curvature of the integral spectrum curve and the signs  $(-)$  and  $(+)$  indicate the decrease or increase of the TGR curve in the case of increasing  $E$ .

The dependence of  $E_{cf}$  on the temperature is demonstrated in Fig. 8 for the energy spectrum shown schematically in Fig. 5. As follows from Fig. 8,

the continuous energy spectrum of rising curvature ( $a > 0$ ) has only a very small effect on the temperature dependence of  $E_{ef}$ , when compared with the effect of the energy spectrum of decreasing curvature ( $a < 0$ ). In the latter case, the  $E_{ef}$  values decrease considerably with rising temperature.

It should be noted that only the value  $(E_{ef})_o$  (i.e. the effective activation energy of the gas diffusion at the onset of heating) may be used for characterization of the energy spectrum  $n(E)$ . The values corresponding to  $(E_{ef})_o$  for the exponential continuous spectra are indicated in Fig. 5 by arrows. For  $a > 0$ , the  $(E_{ef})_o$  depends on the curvature  $a$ , whereas for  $a < 0$  the value  $(E_{ef})_o$  does not appreciably depend on  $a$  and its value is close to the mean value of the exponential spectrum.

The linearized forms of the TGR curves corresponding to the continuous exponential energy spectrum in Fig. 5 are demonstrated in Fig. 9C from which, in the low temperature range, the initial energy of the spectrum can be estimated, in a similar manner to  $(E_{ef})_o$ . In general, however, the curve does not remarkably change with respect to the dependence of the energy spectrum  $n(E)$ .

In a similar way, we have analysed the cases of inert gas release corresponding to the energy spectra characterized by the normal distribution, shown in Fig. 6. The normal distribution spectrum can be expressed

$$\theta(E) = \frac{1}{(2\pi\sigma^2)^{1/2}} \exp\left\{-\left[\frac{E - \bar{E}}{\Delta E}\right]^2 / 2\sigma^2\right\} \quad (13)$$

where  $\sigma$  is the dispersity. The values of  $(E_{ef})_o$  evaluated for the energy spectra are indicated in Fig. 6 by the arrow. The increase of the dispersity  $\sigma$  causes the shift of the  $(E_{ef})_o$  values to the onset of the energy spectrum.

From the analysis of the curves of thermostimulated gas release in the linearized form, we observe that all the energy spectra of normalized shape are characterized by the equal value of the maximum temperature of the peak. This means that all the linearized plots in Figs. 9C and 9D meet at one point where  $U = 0$ . The dotted lines in Figs. 9C and 9D demonstrate the linearized dependences in functional scales for the cases of the discrete energy spectrum with the value  $(E_{ef})_o = 10.5 \text{ kcal mol}^{-1}$ .

## CONCLUSION

We have demonstrated the application of various methods of analysis of the thermostimulated release rate of inert gas from solids, labelled by the diffusion at increased temperature and pressure. The energetic inhomogeneities of the inert gas diffusion sites in solids were revealed using computer simulation of the TGR curves.

## REFERENCES

- 1 I.N. Beckman, A.A. Shviryaev and V. Balek, *Thermochim. Acta*, 104 (1986) 255.
- 2 A.A. Shviryaev, I.N. Beckman and V. Balek, *Thermochim. Acta*, 111 (1987) 217.